IEEE Access
Multidisciplinary | Rapid Review | Open Access Journal

Received December 19, 2018, accepted January 3, 2019, date of publication January 9, 2019, date of current version January 29, 2019.

Digital Object Identifier 10.1109/ACCESS.2019.2891678

Secrecy Performance of Decode-and-Forward Based Hybrid RF/VLC Relaying Systems

JABER AL-KHORI[1], GALYMZHAN NAURYZBAYEV[2], (Member, IEEE), MOHAMED M. ABDALLAH[1], (Senior Member, IEEE), AND MOUNIR HAMDI[1], (Fellow, IEEE)

[1]Division of Information and Computing Technology, College of Science and Engineering, Hamad Bin Khalifa University, Qatar Foundation, Doha, Qatar
[2]Department of Electrical and Computer Engineering, Nazarbayev University, 010000 Astana, Kazakhstan

Corresponding author: Jaber Al-Khori(jalkhori@hbku.edu.qa)

This work was supported in part by the Qatar National Library, and in part by NPRP from the Qatar National Research Fund (a member of Qatar Foundation) under Grant 9-077-2-036.

ABSTRACT In this paper, we consider the secrecy of a hybrid radio frequency (RF)/visible light communication (VLC) system equipped with decode-and-forward relaying. We develop physical layer security algorithms that mitigate eavesdropping on both RF and VLC networks based on zero-forcing beamforming techniques. We evaluate the system performance in terms of secrecy capacity (SC) and outage probability (OP) for two network scenarios, namely non-cooperative (NCPS) and cooperative power saving (CPS) models. The NCPS case assumes fixed power at both source and relay while the CPS case assumes total average power shared between the source and relay. Our objective is to find the minimum power that satisfies a specific SC for both cases. Our simulation results show that CPS policy achieves higher SC and maintain lower OP compared with the NCPS one for the same amount of power. We also show that, for both cases, the hybrid RF/VLC network can improve SC compared with standalone RF or VLC networks.

INDEX TERMS Beamforming (BF), decode-and-forward (DF), maximal ratio combining (MRC), optimization, physical layer security (PLS), radio frequency (RF), relaying, visible light communication (VLC).

I. INTRODUCTION

The rapid growth of the wireless network traffic has led to radio frequency (RF) spectrum congestion. This growth has been driven by new technologies (e.g., Internet-of-Things (IoT), etc. [1]) and the increasing demand of high data-rate mobile broadband applications [2]. The RF spectrum congestion limits the service providers from offering new services [3]. Optical wireless communication (OWC) technologies has recently introduced as an alternative technology that resolves the problem of RF spectrum shortage [4]. Visible light communication (VLC) is a type of OWC system where light can be simultaneously used for illumination and communication purposes in the license-free visible light spectrum range from 430 THz to 790 THz [5]–[7]. This large amount of free bandwidth along with the low complexity of developing the VLC system positioned the technology as a promising alternative for the RF [8]. However, VLC has its own limitations including low coverage and unreliability in the absence of line-of-sight (LOS) [9]. The aforementioned issues can be solved by integrating the both RF and VLC technologies into one hybrid system (known as hybrid RF/VLC) [10]–[13]. This hybrid system has been addressed in the literature where it was shown that RF can offload some part of its traffic in case of the RF congestion to VLC using load balancing strategies [14]. Little and Rahaim [15] describe different mixed and/or hybrid RF/VLC network topologies and discuss their layer link designs. The work in [16] investigates the energy efficiency (EE) while Rakia *et al.* [17] study the optimal data rate maximization with energy harvesting (EH) for mixed VLC/RF relaying systems. Kashef *et al.* [18] study the EE benefits of integrating VLC with RF-based networks where it was shown that the proposed system achieves higher performance compared to the standalone RF system. Another work [19] also focuses on the hybrid RF/VLC relaying system with capabilities of jamming the eavesdroppers. Moreover, Rahaim *et al.* [20] consider an indoor hybrid RF/VLC communication system where VLC broadcast channels are used to support the RF transmission and propose a handover mechanism to optimize the system throughput. Furthermore, it was shown that the proposed system achieves better results in terms of the throughput and delay compared to the standalone RF and/or VLC systems.

A. RELATED WORKS

To enhance the network reliability and improve coverage, it is important to use relays in the both RF and VLC networks [21]–[31]. For instance, Mo *et al.* [21] study the effect of relay placement on the performance of the cell-edge users. The performance, such as outage probability (OP), of decode-and-forward (DF) underlay cognitive radio (CR) relaying systems are investigated in [22] and [23]. On the other hand, Nauryzbayev *et al.* [24] and Arzykulov *et al.* [25] consider the ergodic capacity and the spectral efficiency of amplify-and-forward (AF) relaying networks. Arzykulov *et al.* [26] evaluate the bit-error rate (BER) performance of wireless powered CR relaying networks. Regarding the VLC, the BER performance of relay-assisted full-duplex VLC relaying systems is investigated in [27]. The authors in [28] study the BER performance of OFDM-based relay-assisted VLC systems, where it was shown that the performance can be improved with relay transmission. The work in [29] also investigates the BER performance of full-duplex VLC relaying systems which outperform the ones with direct links. On the other hand, [30] studies a hybrid RF/VLC EH-enabled DF relaying system to increase the system coverage. Rakia *et al.* [31] consider a hybrid RF/VLC system with the EH-based relay under delay constraints where a parameter was developed to control the time for excess EH and data packet retransmission; moreover, it was shown that the parameter has an optimal value able to minimize the packet loss probability.

Wireless data transmission in the RF and VLC systems increases the risk of eavesdropping attacks. Upper layers security techniques, e.g., data encryption, cryptography, etc., can be used to secure the communication, but it typically requires heavy computational and processing powers which result in the high power consumption [32], [33]. On the other hand, physical layer security (PLS) is considered to be a viable solution to secure the communication and prevent the eavesdropping and jamming attacks. Since PLS utilizes the randomness of the communication channels and noise, it can be used to restrict the information reception by an unauthorized user [34]. In [35], to secure the communication, the authors consider the PLS techniques such as diversity-assisted security, physical-layer key generation, artificial-noise-aided security, information-theoretic security, and security-oriented beamforming approaches. For instance, key generation schemes over wireless channels are reviewed in [36], while [37] proposes to use zero-forcing beamforming (ZFBF) strategy to direct the signal away from the eavesdropper in order to achieve the required secrecy rate. Dong *et al.* [38] study various wireless relaying systems with relays following three types of cooperation, namely, DF, AF and cooperative jamming (CJ), where a novel system design was proposed to improve the performance of the wireless PLS. Dong *et al.* [39] consider CJ as an approach to improve the PLS in the practical system design where a suboptimal closed-form solution was proposed to null the jamming signal at the desired destination. Zou *et al.* [40] investigate an optimal relay selection for PLS purposes in cooperative AF- and DF-based wireless networks in order to improve the wireless security against the unauthorized access; moreover, the results show that the proposed solution performs better than the traditional relay selection and also achieves better results compared to multiple-relay combining methods. Liu *et al.* [41] propose a destination-assisted CJ as a PLS method targeting to maximize the secrecy rate.

To the best of the authors' knowledge, the research on the PLS aspects over DF relay-assisted hybrid RF/VLC networks has not been analyzed in the literature. Therefore, in this paper, we consider two different power saving policies, i.e., non-cooperative power saving (NCPS) and cooperative power saving (CPS). For instance, in the case of the NCPS, transmit nodes can be considered as peak-power restricted entities which operate independently without any power cooperation between nodes. On the other hand, the CPS policy describes the other case when the nodes are flexible in terms of the imposed power constraints and only limited by total average power which can be applicable in the following scenario. Since the performance of the DF relaying system is mainly dominated by the weakest channel, it is critical to be able to efficiently distribute the power to maximize the system performance. For instance, the non-utilized power at the source can be used by the relay node to meet this requirement, and vice-versa. To meet the exponentially increasing demands related to the green communications, we formulate the consumed power minimization problem for the both considered subsystems. We investigate the secrecy capacity (SC) region and power consumption achievable under the considered network scenarios. Furthermore, we evaluate the outage performance of the user of interest for both policies.

B. MAIN CONTRIBUTIONS

In this paper, we consider an indoor hybrid RF/VLC DF relaying network and investigate its performance, and our main contributions are as follows:

- We show that the hybrid RF/VLC DF relaying network enhances the performance in terms of secrecy capacity given the same system parameters compared to the standalone RF and VLC systems studied in [18]–[20].
- The CPS policy is proposed for the hybrid RF/VLC DF relaying network to allow the nodes to efficiently share the redundant power in order to improve the confidentiality of the transmission.
- We investigate the performance metrics, such as secrecy capacity, consumed power and secrecy outage probability (SOP), in the presence of the eavesdropper for both NCPS and CPS cases. To achieve perfect secrecy, we exploit the ZFBF technique to prevent the eavesdropping activity and achieve the positive SC for the desired users.
- The SC is evaluated as a function of the predefined SC threshold for the both NCPS and CPS policies. The obtained results demonstrate that the proposed CPS case outperforms the NCPS one, i.e., for the NCPS,

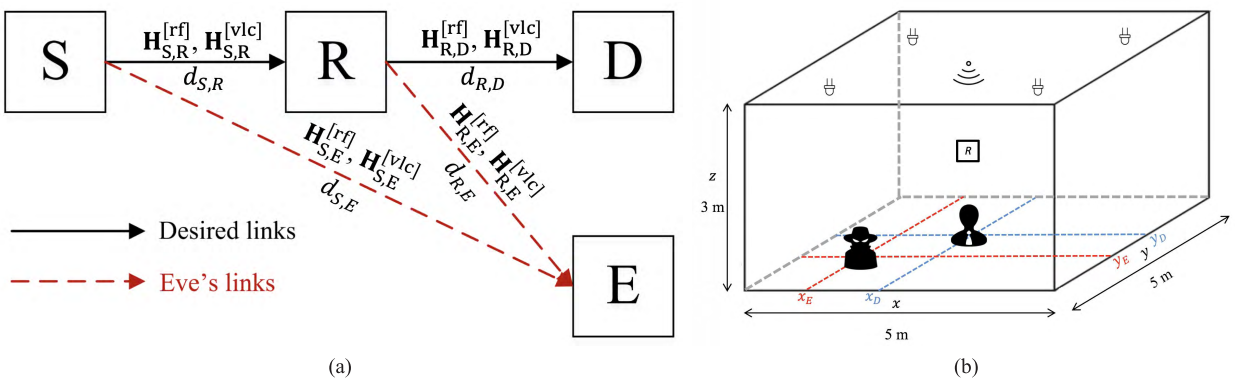

FIGURE 1. An indoor downlink hybrid RF/VLC network scenario. (a) The proposed hybrid RF/VLC network scheme. (b) The room layout.

the SC saturation starts earlier and maximum achievable secrecy is always less than the one obtained for the CPS.
- The results related to the power consumption reveal useful insights into how the power distribution facilitates achieving the required SC by exploiting the non-utilized power. For example, the CPS case ensures that the all available power is used to achieve the given SC which is higher than the one obtainable by the NCPS network.

C. ORGANIZATION AND NOTATION

The rest of the paper is organized as follows. Section II presents the system model of the DF-based hybrid RF/VLC relaying network operating over two time slots. Section III defines the SC as the PLS performance metric. The consumed power minimization problem satisfying the required SC is presented in Section IV. Section V demonstrate the design of beamforming (BF) vectors for the RF and VLC subsystems. Section VI illustrates and discusses the obtained numerical results of our work. Finally, the paper outlines the main concluding remarks in Section VII.

The following notations are used in the paper. Uppercase and lowercase boldfaces are used to denote matrices and vectors, respectively. $(\cdot)^T$ and $(\cdot)^H$ indicate the matrix transpose and matrix conjugate transpose, accordingly. $\mathbb{E}$ and $\mathbb{C}$ stand for the expected value and the complex matrix, respectively. $\sum$ and $\forall$ imply "summation" and "for all" notations, respectively. The acronyms used in the paper are shown in Table 1.

II. SYSTEM MODEL

We consider an indoor downlink hybrid RF/VLC network scenario consisting of the source (S), relay (R), eavesdropper (E) and destination (D) nodes, as shown in Fig. 1. The communication is organized over two transmission time slots (TSs). The first TS is dedicated for the S-to-R communication while the second one is required to maintain the R-to-D transmission, where D is the legitimate receiver which can be characterized by coordinates given by (x_D, y_D, z_D) (see Fig. 1b). Since we assume there is no direct link between the S and D nodes; the information has to be communicated through R within time period T. It is also assumed that E is able to intercept the signals in both TSs as shown in Fig. 1a, and its location is fixed at coordinates (x_E, y_E, z_E) (see Fig. 1b). Moreover, we assume that R operates in the DF mode and each transmit node sends one data stream in the both subsystems, i.e., $l^{[rf]} = l^{[vlc]} = 1$. In the next

TABLE 1. The used acronyms.

Acronym	Definition
AF	Amplify-and-Forward
AWGN	Additive White Gaussian Noise
BF	Beamforming
BER	Bit-Error Rate
CR	Cognitive Radio
CJ	Cooperative Jamming
CPS	Cooperative Power Saving
DF	Decode-and-Forward
DC	Direct Current
EE	Energy Efficiency
EH	Energy Harvesting
FoV	Field-of-View
i.i.d.	independent and identically distributed
IoT	Internet of Things
KKT	Karush-Kuhn-Tucker
LOS	Line-Of-Sight
MRC	Maximal Ratio Combining
MIMO	Multiple-Input Multiple-Output
NCPS	Non-Cooperative Power Saving
OWC	Optical Wireless Communication
OP	Outage Probability
PD	Photo-Detector
PLS	Physical Layer Security
RF	Radio Frequency
SC	Secrecy Capacity
SNR	Signal-to-Noise Ratio
SOP	Secrecy Outage Probability
TS	Time Slot
VLC	Visible Light Communication
ZFBF	Zero-Forcing Beamforming

subsections, we will describe the system model with respect to the RF and VLC subsystems.

A. THE RF SUBSYSTEM

In the first TS, S transmits the message x_S to R which forwards the decoded signal x_R ($x_R = \tilde{x}_S$) to D within the second TS. Therefore, the received signal at node i can be expressed as

$$\mathbf{y}_i^{[\mathrm{rf}]}(t) = \sqrt{\frac{P_j^{[\mathrm{rf}]}}{d_{j,i}^{[\mathrm{rf}]\tau}}}\mathbf{H}_{j,i}^{[\mathrm{rf}]}\mathbf{w}_j^{[\mathrm{rf}]}x_j(t) + \mathbf{n}_i^{[\mathrm{rf}]}(t), \tag{1}$$

where $\mathbf{H}_{j,i}^{[\mathrm{rf}]} \in \mathbb{C}^{M_j^{[\mathrm{rf}]} \times M_i^{[\mathrm{rf}]}}$ denotes the channel matrix between transmitter $j \in \{S, R\}$, and receiver $i \in \{R, D\}$, and we assume that each channel coefficient is drawn from independent and identically distributed (i.i.d.) statistical model according to $\mathcal{CN}(0, 1)$ and each channel is frequency flat fading and remains constant during each TS [37]. We assume that all nodes are equipped with multiple antennas and $M_{(\cdot)}$ represents the number of deployed antennas.[1] $P_j^{[\mathrm{rf}]} \leq P_{j_{\max}}^{[\mathrm{rf}]}$ is the transmit power from transmitter j. $d_{j,i}^{[\mathrm{rf}]}$ represents the distance between the jth and ith nodes, and τ denotes the path loss exponent. $\mathbf{w}_j^{[\mathrm{rf}]} \in \mathbb{C}^{M_j \times 1}$ is the BF vector employed at transmitter j, where $\mathbb{C}$ stands for a complex matrix. $\mathbf{n}_i^{[\mathrm{rf}]}$ denotes the zero-mean additive white Gaussian noise (AWGN) at receiver i with variance $\sigma_{n_i}^{[\mathrm{rf}]2}$. For the sake of simplicity, we omit time indexing in the following equations.

At the same time, E attempts to intercept the desired message transmitted from the source to the legitimate receiver, and the corresponding received signal at E during the both TSs can be expressed as

$$\mathbf{y}_{j,E}^{[\mathrm{rf}]} = \sqrt{\frac{P_j^{[\mathrm{rf}]}}{d_{j,E}^{[\mathrm{rf}]\tau}}}\mathbf{H}_{j,E}^{[\mathrm{rf}]}\mathbf{w}_j^{[\mathrm{rf}]}x_j + \mathbf{n}_E^{[\mathrm{rf}]}, \quad j \in \{S, R\}, \tag{2}$$

where $\mathbf{H}_{j,E}^{[\mathrm{rf}]} \in \mathbb{C}^{M_j \times M_E^{[\mathrm{rf}]}}$ denotes the channel matrix observed by E from transmitter j, and $d_{j,E}^{[\mathrm{rf}]}$ stands for the distance between transmitter j and E. $\mathbf{n}_E^{[\mathrm{rf}]}$ indicates the AWGN noise at E, with variance $\sigma_{n_E}^{[\mathrm{rf}]2}$.

B. THE VLC SUBSYSTEM

In this section, we consider the VLC source and relay nodes consisting of a number of LEDs driven by a constant direct current (DC) bias current $I^{[\mathrm{vlc}]}$. These nodes have information encoders that code the initial data bits to produce z which is superimposed on $I^{[\mathrm{vlc}]}$ to generate the compound current signal $I^{[\mathrm{vlc}]} + z$ to be transmitted over the air. It is worthwhile mentioning that, compared to the RF subsystem, VLC communication is limited by an amplitude constraint given by $|z| \leq \epsilon I^{[\mathrm{vlc}]}$, $\epsilon \in [0, 1]$, to avoid a non-linear current-light conversion region at the transmit nodes [42]. The instantaneous generated optical power can be written as $P_{opt}^{[\mathrm{vlc}]} = k^{[\mathrm{vlc}]}(I^{[\mathrm{vlc}]} + z)$, where $k^{[\mathrm{vlc}]}$ (Watt/A) is the conversion efficiency factor depending on the LED properties.

Therefore, the optical signal can be transmitted through a channel $\mathbf{H}_{j,i}^{[\mathrm{vlc}]}$, $i \in \{R, D\}$, $j \in \{S, R\}$, given by a set of channel coefficients $h^{[\mathrm{vlc}]}$ modeled as [43]

$$h^{[\mathrm{vlc}]} = \begin{cases} \dfrac{(m+1)A}{2\pi d^2}\cos^m\phi T_s(\psi)g(\psi)\cos\psi, & 0 \leq \psi \leq \Psi_c, \\ 0, & \theta > \Psi_c, \end{cases} \tag{3}$$

where A denotes the physical detector area. m stands for the order of Lambertian emission with a half irradiance semi-angle of $\phi_{\frac{1}{2}}$. d represents the distance from the transmitter to the receiver. ϕ and ψ represent the angle of irradiance and the angle of incidence with respect to the receiver axis, respectively. Ψ_c, $g(\psi)$, and $T_s(\psi)$ represent the concentrator field-of-view (FOV), the concentrator gain and the signal transmission of the filter, respectively.

The received signal at node i can be written as

$$\mathbf{y}_i^{[\mathrm{vlc}]} = \rho_i\kappa_j N_j\mathbf{H}_{j,i}^{[\mathrm{vlc}]}\mathbf{w}_j^{[\mathrm{vlc}]}z_j + \mathbf{n}_i^{[\mathrm{vlc}]}, \tag{4}$$

where ρ_i denotes the responsivity of the photo-detector (PD). κ_j and N_j stand for the scaling factor (depending on the LED model) and the number of LEDs per each light fixture, respectively. $\mathbf{H}_{j,i}^{[\mathrm{vlc}]}$ represents the channel link between transmitter $j \in \{S, R\}$ and receiver $i \in \{R, D\}$ and $\mathbf{w}_j^{[\mathrm{vlc}]}$ is the BF vector. Due to the DF mode, the relay transmit signal z_R is the decoded version of the signal z_S while $\mathbf{n}_i^{[\mathrm{vlc}]}$ stands for AWGN noise terms with variance $\sigma_{n_i}^{[\mathrm{vlc}]2}$.

At the same time, the received signal at E during both phases can be expressed as,

$$\mathbf{y}_{j,E}^{[\mathrm{vlc}]} \ \rho_E\kappa_j N_j\mathbf{H}_{j,E}^{[\mathrm{vlc}]}\mathbf{w}_j^{[\mathrm{vlc}]}z_j + \mathbf{n}_E^{[\mathrm{vlc}]}, \quad j \in \{S, R\}, \tag{5}$$

where ρ_E stands for the PD responsivity. $\mathbf{H}_{j,E}^{[\mathrm{vlc}]}$ denotes the channel link between transmitter j and eavesdropper E. $\mathbf{n}_E^{[\mathrm{vlc}]}$ denotes the AWGN noise term with variances $\sigma_{n_E}^{[\mathrm{vlc}]2}$.

III. SECRECY CAPACITY

In this section, we evaluate the performance of the hybrid RF/VLC network scenario in terms of the secrecy capacity (Δ) which represents the difference between the channel capacity of the authorized receiver and the capacity achievable by the illegitimate user [44]. To effectively exploit the available channel gains, we deploy multiple-input multiple-output (MIMO) maximal ratio combining (MRC) technique [45] for the both RF and VLC subsystems. Therefore, the effective channel gain can be represented as a sum of all receive signal branches.

[1] Note that we set $M = 4$ antennas in order to satisfy the minimum feasibility conditions imposed by the deployed joint zero-forcing beamforming and SNR maximization scheme.

A. THE RF-BASED SECRECY CAPACITY

The signal-to-noise ratio (SNR) for the signal given in (1) can be written as

$$\gamma_i^{[\mathrm{rf}]} = \frac{P_j^{[\mathrm{rf}]} \sum_{m=1}^{M} |\mathbf{H}_{j,i}^{[\mathrm{rf}]}(m)\mathbf{w}_j^{[\mathrm{rf}]}|^2}{d_{j,i}^{[\mathrm{rf}]\tau}\sigma_{n_i}^{[\mathrm{rf}]2}}, \quad i \in \{R, D\},\ j \in \{S, R\}, \tag{6}$$

where the effective channel gains are summarized by using MRC. $\mathbf{H}_{j,i}^{[\mathrm{rf}]}(m)$ represents the m^{th} row of $\mathbf{H}_{j,i}^{[\mathrm{rf}]}$. On the other hand, the SNR at E can be given as

$$\gamma_{j,E}^{[\mathrm{rf}]} = \frac{P_j^{[\mathrm{rf}]} \sum_{m=1}^{M} |\mathbf{H}_{j,E}^{[\mathrm{rf}]}(m)\mathbf{w}_j^{[\mathrm{rf}]}|^2}{d_{j,E}^{[\mathrm{rf}]\tau}\sigma_{n_E}^{[\mathrm{rf}]2}}, \quad j \in \{S, R\}. \tag{7}$$

Due to the considered DF relaying, the instantaneous end-to-end capacity can be written as

$$C^{[\mathrm{rf}]} = \frac{1}{2}\log_2\left(1 + \min\left(\gamma_R^{[\mathrm{rf}]}, \gamma_D^{[\mathrm{rf}]}\right)\right). \tag{8}$$

On the other hand, the channel capacity of E can be expressed as

$$C_{j,E}^{[\mathrm{rf}]} = \frac{1}{2}\log_2\left(1 + \gamma_{j,E}^{[\mathrm{rf}]}\right), \quad j \in \{S, R\}. \tag{9}$$

To achieve perfect secrecy, the transmitter and legitimate user should communicate at a positive rate while nulling the data delivery toward E [46]. The SC conditions for the S-to-R and R-to-D communication links can be respectively expressed as

$$\Delta_i^{[\mathrm{rf}]} = C_i^{[\mathrm{rf}]} - C_{j,E}^{[\mathrm{rf}]} \geq 0, \quad i \in \{R, D\},\ j \in \{S, R\}, \tag{10}$$

where $C_i^{[\mathrm{rf}]} = \frac{1}{2}\log_2\left(1 + \gamma_i^{[\mathrm{rf}]}\right)$.

To satisfy the condition in (10), we evaluate the SC by subtracting the maximum channel capacity of E from the efficient RF-based capacity of the user of interest as follows

$$\begin{aligned}\Delta^{[\mathrm{rf}]} &= C^{[\mathrm{rf}]} - \max\left(C_{S,E}^{[\mathrm{rf}]}, C_{R,E}^{[\mathrm{rf}]}\right)\\ &= \frac{1}{2}\log_2\left(1 + \min\left(\gamma_R^{[\mathrm{rf}]}, \gamma_D^{[\mathrm{rf}]}\right)\right)\\ &\quad - \frac{1}{2}\log_2\left(1 + \max\left(\gamma_{S,E}^{[\mathrm{rf}]}, \gamma_{R,E}^{[\mathrm{rf}]}\right)\right)\\ &= \log_2\left(\left(\frac{1 + \min\left(\gamma_R^{[\mathrm{rf}]}, \gamma_D^{[\mathrm{rf}]}\right)}{1 + \max\left(\gamma_{S,E}^{[\mathrm{rf}]}, \gamma_{R,E}^{[\mathrm{rf}]}\right)}\right)^{\frac{1}{2}}\right) \geq 0.\end{aligned} \tag{11}$$

The condition (11) can be satisfied by following

$$\min(\gamma_R^{[\mathrm{rf}]}, \gamma_D^{[\mathrm{rf}]}) \geq \max(\gamma_{S,E}^{[\mathrm{rf}]}, \gamma_{R,E}^{[\mathrm{rf}]}). \tag{12}$$

It is shown by using ZFBF the SC is close to be optimal which ensures nulling the rate of E. ZFBF ensures $\mathbf{H}_{j,E}^{[\mathrm{rf}]}\mathbf{w}_j^{[\mathrm{rf}]} = 0$, $j \in \{S, R\}$. As a result, $\gamma_{j,E}^{[\mathrm{rf}]} = 0$, and the condition in (12) can be simplified as

$$\min(\gamma_R^{[\mathrm{rf}]}, \gamma_D^{[\mathrm{rf}]}) \geq 0. \tag{13}$$

B. THE VLC-BASED SECRECY CAPACITY

The transmit power is given as

$$P_{tx_j}^{[\mathrm{vlc}]} = P_j^{[\mathrm{vlc}]} N_j^2 \mathbf{w}_j^{[\mathrm{vlc}]T}\mathbf{w}_j^{[\mathrm{vlc}]}, \quad j \in \{S, R\}, \tag{14}$$

where $P_j^{[\mathrm{vlc}]}$ is the average consumed electrical power per LED, with $\mathbb{E}\{|z_j|^2\} = P_j^{[\mathrm{vlc}]}$ where $\mathbb{E}\{\cdot\}$ represents the expected value.

On the other hand, the received power levels during both phases are represented as

$$P_{rx_i}^{[\mathrm{vlc}]} = \left(\rho_i N_j \kappa_j \sum_{f=1}^{F} \mathbf{H}_{j,i}^{[\mathrm{vlc}]}(f)^T \mathbf{w}_j^{[\mathrm{vlc}]}\right)^2 P_j^{[\mathrm{vlc}]}, \tag{15}$$

where $\mathbf{H}_{j,i}^{[\mathrm{vlc}]}(f)^T$ represents the m^{th} row of $\mathbf{H}_{j,i}^{[\mathrm{vlc}]T}$, $i \in \{R, D\}, j \in \{S, R\}$.

The received power levels at E during both phases are represented for $j \in \{S, R\}$ as

$$P_{rx_{j,E}}^{[\mathrm{vlc}]} = \left(\rho_E N_j \kappa_j \sum_{f=1}^{F} \mathbf{H}_{j,E}^{[\mathrm{vlc}]}(f)^T \mathbf{w}_j^{[\mathrm{vlc}]}\right)^2 P_j^{[\mathrm{vlc}]}. \tag{16}$$

The SNR value for the signal given in (4) can be written as

$$\gamma_i^{[\mathrm{vlc}]} = \frac{P_{rx_i}^{[\mathrm{vlc}]}}{\sigma_{n_i}^{[\mathrm{vlc}]2}}, \quad i \in \{R, D\}, \tag{17}$$

while the SNR values at E for both phases are given by

$$\gamma_{j,E}^{[\mathrm{vlc}]} = \frac{P_{rx_{j,E}}^{[\mathrm{vlc}]}}{\sigma_{n_E}^{[\mathrm{vlc}]2}}, \quad j \in \{S, R\}. \tag{18}$$

Due to the considered DF relaying, the instantaneous end-to-end capacity can be written as

$$C^{[\mathrm{vlc}]} = \frac{1}{2}\log_2\left(1 + \min\left(\frac{2\gamma_R^{[\mathrm{vlc}]}}{\pi e}, \frac{2\gamma_D^{[\mathrm{vlc}]}}{\pi e}\right)\right), \tag{19}$$

On the other hand, the channel capacity of E can be given by

$$C_{j,E}^{[\mathrm{vlc}]} = \frac{1}{2}\log_2\left(1 + \frac{2\gamma_{j,E}^{[\mathrm{vlc}]}}{\pi e}\right), \quad j \in \{S, R\}. \tag{20}$$

Similar to Section III-A, we define the VLC-based SC for the S-to-R and R-to-D communication sessions as

$$\Delta_i^{[\mathrm{vlc}]} = C_i^{[\mathrm{vlc}]} - C_{j,E}^{[\mathrm{vlc}]} \geq 0, \quad i \in \{R, D\},\ j \in \{S, R\}, \tag{21}$$

where $C_i^{[\mathrm{vlc}]} = \frac{1}{2}\log_2\left(1 + \frac{2\gamma_i^{[\mathrm{vlc}]}}{\pi e}\right)$.

To satisfy the condition in (21), we evaluate the SC by subtracting the maximum channel capacity of E from the efficient VLC-based capacity of the user of interest as follows

$$\begin{aligned}\Delta^{[\mathrm{vlc}]} &= C^{[\mathrm{vlc}]} - \max\left(C_{S,E}^{[\mathrm{vlc}]}, C_{R,E}^{[\mathrm{vlc}]}\right)\\ &= \frac{1}{2}\log_2\left(1 + \min\left(\frac{2\gamma_R^{[\mathrm{vlc}]}}{\pi e}, \frac{2\gamma_D^{[\mathrm{vlc}]}}{\pi e}\right)\right)\end{aligned}$$

Algorithm 1 The NCPS Policy

Require:

inputs $\mathbf{H}_{j,k}^{[i]}, \mathbf{H}_{j,E}^{[i]}, P_{j\max}^{[i]}, \ \Delta_{\text{th}}, \alpha, N_j \ \forall i \in \{\text{rf}, \text{vlc}\}, j \in \{S, R\}, k \in \{R, D\}$

Ensure:

This part is dedicated for the RF subsystem design

for j **do**

  if (27b) && (27c) are TRUE using Lagrangian duality and KKT conditions **then**

    calculate $\mathbf{w}_j^{[\text{rf}]}$ according to (27a)

  end if

  return $\mathbf{w}_j^{[\text{rf}]}$.

end for

This part is dedicated for the VLC subsystem design

for j **do**

  if (32b) && (32c) are TRUE using linear programming optimizer **then**

    calculate $\mathbf{w}_j^{[\text{vlc}]}$ according to (32a)

  end if

  return $\mathbf{w}_j^{[\text{vlc}]}$.

end for

These derived vectors $\mathbf{w}_j^{[\text{rf}]}$ *and* $\mathbf{w}_j^{[\text{vlc}]}$ *will be used in the next iteration*

if $C^{[\text{rf}]} + C^{[\text{vlc}]} \geq \Delta_{\text{th}}$ && $P_j^{[\text{rf}]} \leq P_{j\max}^{[\text{rf}]}$ && $P_j^{[\text{vlc}]} \leq P_{j\max}^{[\text{vlc}]}$ **then**

  calculate the consumed power according to (25a)

end if

return $P_j^{[\text{rf}]}, P_j^{[\text{vlc}]}, C^{[\text{rf}]}, C^{[\text{vlc}]}$.

$$-\frac{1}{2}\log_2\left(1+\max\left(\frac{2\gamma_{S,E}^{[\text{vlc}]}}{\pi e},\frac{2\gamma_{R,E}^{[\text{vlc}]}}{\pi e}\right)\right) = \log_2\left(\left(\frac{1+\min\left(\frac{2\gamma_R^{[\text{vlc}]}}{\pi e},\frac{2\gamma_D^{[\text{vlc}]}}{\pi e}\right)}{1+\max\left(\frac{2\gamma_{S,E}^{[\text{vlc}]}}{\pi e},\frac{2\gamma_{R,E}^{[\text{vlc}]}}{\pi e}\right)}\right)^{\frac{1}{2}}\right) \geq 0. \tag{22}$$

The condition (22) can be satisfied by following

$$\min\left(\gamma_R^{[\text{vlc}]}, \gamma_D^{[\text{vlc}]}\right) \geq \max\left(\gamma_{S,E}^{[\text{vlc}]}, \gamma_{R,E}^{[\text{vlc}]}\right). \tag{23}$$

By using the ZFBF in the VLC subsystem, the SC is close to be optimal which ensures nulling the data at E. ZFBF ensures $\mathbf{H}_{j,E}^{[\text{vlc}]T}\mathbf{w}_j^{[\text{vlc}]} = 0, \ j \in \{S, R\}$ at E. As a result, $\gamma_{j,E}^{[\text{vlc}]} = 0$ and the condition (23) can be simplified as

$$\min\left(\gamma_R^{[\text{vlc}]}, \gamma_D^{[\text{vlc}]}\right) \geq 0. \tag{24}$$

IV. PROBLEM FORMULATION

In this section, we define the EE maximization problem, where EE is given as the sum of the achieved data rate per consumed power unit (bits/s/Hz/Watt). We design the transmit BF vectors to maximize the EE of the hybrid RF/VLC network over the assigned transmission power levels. The total achieved SC, namely, $C^{[\text{vlc}]} + C^{[\text{RF}]}$, is constrained by the minimum required SC. Our goal is to secure the S-to-R and R-to-D communication links with the presence of E by using ZFBF as the PLS technique to prevent the data transmission to E. Moreover, our target is to minimize the weighted sum of the consumed electrical power in the considered hybrid RF/VLC relaying network. This problem can be solved in terms of different power saving policies, i.e., non-cooperative and cooperative ones.

A. NON-COOPERATIVE POWER SAVING POLICY

The NCPS policy allows one to assign predefined power levels to certain transmit nodes in the both VLC and RF subsystems. With this in mind, we aim to minimize the total consumed power while achieving the required SC as

$$\underset{\forall P_j^{[i]}, \boldsymbol{w}_j^{[i]}}{\textit{minimize}} \ \alpha N^2\left(\mathbf{w}_S^{[\text{vlc}]T}\mathbf{w}_S^{[\text{vlc}]}P_S^{[\text{vlc}]} + \mathbf{w}_R^{[\text{vlc}]T}\mathbf{w}_R^{[\text{vlc}]}P_R^{[\text{vlc}]}\right) + (1-\alpha)\left(\mathbf{w}_S^{[\text{rf}]H}\mathbf{w}_S^{[\text{rf}]}P_S^{[\text{rf}]} + \mathbf{w}_R^{[\text{rf}]H}\mathbf{w}_R^{[\text{rf}]}P_R^{[\text{rf}]}\right) \tag{25a}$$

$$\text{subject to } C^{[\text{rf}]} + C^{[\text{vlc}]} \geq \Delta_{\text{th}}, \tag{25b}$$

$$P_j^{[\text{i}]} \leq P_{j_{\max}}^{[\text{i}]}, \tag{25c}$$

$$\sum_{m=1}^{M}\mathbf{H}_{j,E}^{[\text{rf}]}(m)\mathbf{w}_j^{[\text{rf}]} = 0, \tag{25d}$$

$$\sum_{f=1}^{F}\mathbf{H}_{j,E}^{[\text{vlc}]}(f)^T\mathbf{w}_j^{[\text{vlc}]} = 0, \tag{25e}$$

$$-1 \leq \mathbf{w}_j^{[\text{vlc}]} \leq 1, \tag{25f}$$

$$\mathbf{w}_j^{[\text{rf}]H}\mathbf{w}_j^{[\text{rf}]} \leq 1, \tag{25g}$$

where $i \in \{\text{vlc}, \text{rf}\}$ and $j \in \{S, R\}$. $0 \leq \alpha \leq 1$ denotes the coefficient defining which technology, RF or VLC, is given a more priority in the power minimization where Δ_{th} represents the total required SC. The constraint (25b) is needed to achieve the required SC while the power constraint is given by (25c). The constraints (25d) and (25e) are to satisfy the ZFBF conditions by nulling out the directions to E, respectively. The constraints (25f) and (25g) maintain the power unity of the RF and VLC subsystems, and these BF vectors will be obtained in Section V. The power minimization problem can be solved by following Algorithm 1.

B. COOPERATIVE POWER SAVING POLICY

It is worthwhile mentioning that the CPS policy also assigns the predefined amount of power to the transmit nodes as the NCPS does. However, the CPS can be characterized by an additional degree of freedom given by an opportunity of power sharing, e.g., if S has some non-used power and R is lack of the power to maintain the required SC, this power can be effectively used by R. Therefore, the consumed power minimization problem can be written as

$$\underset{\forall P_j^{[i]}, \boldsymbol{w}_j^{[i]}}{\textit{minimize}} \ \alpha N^2\left(\mathbf{w}_S^{[\text{vlc}]T}\mathbf{w}_S^{[\text{vlc}]}P_S^{[\text{vlc}]} + \mathbf{w}_R^{[\text{vlc}]T}\mathbf{w}_R^{[\text{vlc}]}P_R^{[\text{vlc}]}\right)$$

$$+(1-\alpha)\left(\mathbf{w}_S^{[\mathrm{rf}]H}\mathbf{w}_S^{[\mathrm{rf}]}P_S^{[\mathrm{rf}]}+\mathbf{w}_R^{[\mathrm{rf}]H}\mathbf{w}_R^{[\mathrm{rf}]}P_R^{[\mathrm{rf}]}\right) \tag{26a}$$

$$\text{subject to } C^{[\mathrm{rf}]}+C^{[\mathrm{vlc}]}\geq\Delta_{\mathrm{th}}, \tag{26b}$$

$$0\leq\sum_j P_j^{[\mathrm{i}]}\leq P_{j_{\max}}^{[\mathrm{i}]}, \tag{26c}$$

$$\sum_{m=1}^{M}\mathbf{H}_{j,E}^{[\mathrm{rf}]}(m)\mathbf{w}_j^{[\mathrm{rf}]}=0, \tag{26d}$$

$$\sum_{f=1}^{F}\mathbf{H}_{j,E}^{[\mathrm{vlc}]}(f)^T\mathbf{w}_j^{[\mathrm{vlc}]}=0, \tag{26e}$$

$$-1\leq\mathbf{w}_j^{[\mathrm{vlc}]}\leq 1, \tag{26f}$$

$$\mathbf{w}_j^{[\mathrm{rf}]H}\mathbf{w}_j^{[\mathrm{rf}]}\leq 1, \tag{26g}$$

where $i\in\{\mathrm{vlc},\mathrm{rf}\}$ and $j\in\{S,R\}$. $0\leq\alpha\leq 1$ denotes the coefficient defining which technology, RF or VLC, is given a more priority in the power minimization where Δ_{th} represents the total required SC. The constraint (26b) is needed to achieve the required SC. The constraint (26c) is necessary to ensure the power distribution between the transmit nodes. The constraints (26d) and (26e) are to satisfy the ZFBF conditions by nulling out the directions to E, respectively. The constraints (26f) and (26g) maintain the power unity requirement for the RF and VLC subsystems, and these BF vectors will be obtained in Section V. The power minimization problem can be solved by following Algorithm 2.

Algorithm 2 The CPS Policy

Require:

inputs $\mathbf{H}_{j,k}^{[i]}, \mathbf{H}_{j,E}^{[i]}, P_{j\max}^{[i]}$, $\Delta_{\mathrm{th}}, \alpha, N_j\ \forall i\in\{\mathrm{rf},\mathrm{vlc}\}, j\in\{S,R\}, k\in\{R,D\}$

Ensure:

This part is dedicated for the RF subsystem design

for j **do**

  if (27b) && (27c) are TRUE using Lagrangian duality and KKT conditions **then**

    calculate $\mathbf{w}_j^{[\mathrm{rf}]}$ according to (27a)

  end if

  return $\mathbf{w}_j^{[\mathrm{rf}]}$.

end for

This part is dedicated for the VLC subsystem design

for j **do**

  if (32b) && (32c) are TRUE using linear programming optimizer **then**

    calculate $\mathbf{w}_j^{[\mathrm{vlc}]}$ according to (32a)

  end if

  return $\mathbf{w}_j^{[\mathrm{vlc}]}$.

end for

These derived vectors $\mathbf{w}_j^{[\mathrm{rf}]}$ *and* $\mathbf{w}_j^{[\mathrm{vlc}]}$ *will be used in the next iteration*

if $C^{[\mathrm{rf}]}+C^{[\mathrm{vlc}]}\geq\Delta_{\mathrm{th}}$ && $\sum_j P_j^{[\mathrm{rf}]}\leq P_{\max}^{[\mathrm{rf}]}$ && $\sum_j P_j^{[\mathrm{vlc}]}\leq P_{\max}^{[\mathrm{vlc}]}$ **then**

  calculate the consumed power according to (26a)

end if

return $P_j^{[\mathrm{rf}]}, P_j^{[\mathrm{vlc}]}, C^{[\mathrm{rf}]}, C^{[\mathrm{vlc}]}$.

V. BEAMFORMING DESIGN

A. RF BEAMFORMING

Since we consider a dual-hop network scenario, we have to obtain two sets of the BF weights. The optimization that maximizes the channel gain of the S-to-R and R-to-D links while securing communication from E can be given as

$$\underset{\mathbf{w}_j^{[\mathrm{rf}]}}{\mathit{maximize}}\ \sum_{m=1}^{M}\mathbf{H}_{j,i}^{[\mathrm{rf}]}(m)\mathbf{w}_j^{[\mathrm{rf}]},\ i\in\{R,D\} \tag{27a}$$

$$\text{subject to } \sum_{m=1}^{M}\mathbf{H}_{j,E}^{[\mathrm{rf}]}(m)\mathbf{w}_j^{[\mathrm{rf}]}=0, \tag{27b}$$

$$\mathbf{w}_j^{[\mathrm{rf}]H}\mathbf{w}_j^{[\mathrm{rf}]}\leq 1,\quad j\in\{S,R\}. \tag{27c}$$

The objective function in (27a) is linear and the given constraints are convex. So it is a convex optimization problem that can be solved via Lagrangian duality [47]. The objective and constraint functions can be written as

$$L_{j,i}=-\sum_{m=1}^{M}\mathbf{H}_{j,i}^{[\mathrm{rf}]}(m)\mathbf{w}_j^{[\mathrm{rf}]}+\zeta_{j,i}(\mathbf{w}_j^{[\mathrm{rf}]H}\mathbf{w}_j^{[\mathrm{rf}]}-1)+\eta_{j,i}\sum_{m=1}^{M}\mathbf{H}_{j,E}^{[\mathrm{rf}]}(m)\mathbf{w}_j^{[\mathrm{rf}]},\quad i\in\{R,D\},\ j\in\{S,R\}, \tag{28}$$

where $\zeta_{j,i}$ and $\eta_{j,i}$ are the Lagrangian multipliers. By applying Karush-Kuhn-Tucker (KKT) conditions [47], the optimum RF BF vectors for the first phase can be obtained as

$$\mathbf{w}_j^{[\mathrm{rf}]}=\frac{\sum_{m=1}^{M}\mathbf{H}_{j,i}^{[\mathrm{rf}]}(m)^H-\eta_{j,i}\sum_{m=1}^{M}\mathbf{H}_{j,E}^{[\mathrm{rf}]}(m)^H}{2\zeta_{j,i}}, \tag{29}$$

where $i\in\{R,D\}$, $j\in\{S,R\}$. Using Lagrangian duality and applying the KKT conditions, the optimum values of Lagrangian multipliers can be found as

$$\zeta_{j,i}=\sqrt{\frac{\beta_{j,i}^{[1]}-\beta_{j,i}^{[2]}-\beta_{j,i}^{[3]}+\beta_{j,i}^{[4]}}{4}},\quad i\in\{R,D\},\ j\in\{S,R\}, \tag{30}$$

where $\beta_{j,i}^{[1]}=\sum_{m=1}^{M}\mathbf{H}_{j,i}^{[\mathrm{rf}]}(m)\sum_{m=1}^{M}\mathbf{H}_{j,i}^{[\mathrm{rf}]}(m)^H$, $\beta_{j,i}^{[2]}=\eta_{j,i}\sum_{m=1}^{M}\mathbf{H}_{j,i}^{[\mathrm{rf}]}(m)\sum_{m=1}^{M}\mathbf{H}_{j,E}^{[\mathrm{rf}]}(m)^H$, $\beta_{j,i}^{[3]}=\eta_{j,i}\sum_{m=1}^{M}\mathbf{H}_{j,E}^{[\mathrm{rf}]}(m)\sum_{m=1}^{M}\mathbf{H}_{j,i}^{[\mathrm{rf}]}(m)^H$ and $\beta_{j,i}^{[4]}=\eta_{j,i}^2\sum_{m=1}^{M}\mathbf{H}_{j,E}^{[\mathrm{rf}]}(m)\sum_{m=1}^{M}\mathbf{H}_{j,E}^{[\mathrm{rf}]}(m)^H$, and

$$\eta_{j,i}=\frac{\sum_{m=1}^{M}\mathbf{H}_{j,E}^{[\mathrm{rf}]}(m)\sum_{m=1}^{M}\mathbf{H}_{j,i}^{[\mathrm{rf}]}(m)^H}{\sum_{m=1}^{M}\mathbf{H}_{j,E}^{[\mathrm{rf}]}(m)\sum_{m=1}^{M}\mathbf{H}_{j,E}^{[\mathrm{rf}]}(m)^H}, \tag{31}$$

where $i\in\{R,D\}$, $j\in\{S,R\}$.

B. VLC BEAMFORMING

In this section, we derive two sets of the VLC BF weights to maximize the achievable SC. we define the maximization

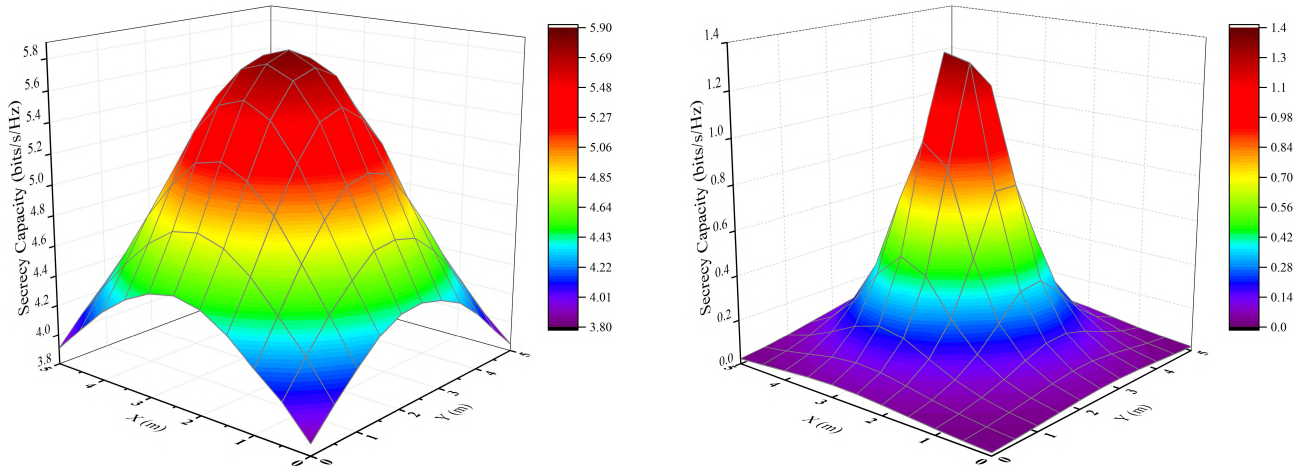

FIGURE 2. The achievable secrecy capacity of the standalone RF and VLC systems with respect to the room dimensions in the presence of E. (a) RF SC. (b) VLC SC.

problem follows

$$\underset{\mathbf{w}_j^{[\text{vlc}]}}{\textit{maximize}} \sum_{f=1}^{F} \mathbf{H}_{j,i}^{[\text{vlc}]}(f)^T \mathbf{w}_j^{[\text{vlc}]}, \ i \in \{R, D\} \quad (32a)$$

$$\text{subject to} \sum_{f=1}^{F} \mathbf{H}_{j,E}^{[\text{vlc}]}(f)^T \mathbf{w}_j^{[\text{vlc}]} = 0, \quad (32b)$$

$$-1 \leq \mathbf{w}_j^{[\text{vlc}]} \leq 1, \quad j \in \{S, R\}. \quad (32c)$$

The problem in (32a) can be solved using any linear programming optimizer (e.g., `fmincon` MATLAB function) which will ensure that the desired signal will be canceled at E given by (32b) and the obtained VLC BF vectors will satisfy the power constraint (32c).

VI. SIMULATION RESULTS

This section presents some numerical results on the physical layer security aspects for the indoor hybrid RF/VLC networks in the presence of the unauthorized user. To be more specific, we consider the non-cooperative and cooperative power distribution scenarios where we apply the ZFBF technique to mitigate the signal reception at E. In this section, we also estimate the consumed power required to satisfy the secrecy capacity threshold, Δ_{th}, set equal to 6 bits/s/Hz[2] for the both considered cases. Moreover, the RF and VLC parameters are depicted in Tables 2 and 3, respectively. The weighting factor α in Eqs. (25a) and (26a) is equal to 0.5. We assume that the legitimate user moves within the indoor environment with dimensions of 5m × 5m × 3m (see Fig. 1b) while the E's location is kept fixed at (2, 2, 1.9) m. It is also worth mentioning that the standalone RF and VLC systems are chosen as the benchmark technologies to evaluate the system performance of the proposed techniques.

[2]Note that we set $\Delta_{\text{th}} = 6$ bits/s/Hz to evaluate the ultimate performance of the proposed model based on the selected system parameters given in Tables 2 and 3.

TABLE 2. The RF simulation parameters.

Parameter	Value
The location of S	$(x = 2.5, y = 2.5, z = 3)$ m
The location of R	$(x = 2.5, y = 2.5, z = 2)$ m
Available power per node j, $P_{j_{max}}$, $j \in \{R, D, E\}$	1 Watt
Noise power per node i, $\sigma_{n_i}^2$, $i \in \{R, D, E\}$	10^{-3} Watt
Number of antennas, M_i, $i \in \{S, R, D, E\}$	4
Path loss exponent (τ)	2.7

In Fig. 2, we plot the achievable secrecy capacity of the standalone RF and VLC systems with the same network parameters. Based on the results, we can see that both standalone systems can not reach the required secrecy capacity threshold of 6 bits/s/Hz, i.e., the user in the center of the room achieves 5.9 bits/s/Hz and 1.4 bits/s/Hz for the standalone RF and VLC models, respectively. Therefore, it is reasonable to integrate these technologies into one hybrid system in order to enhance the secrecy performance of the network without extra infrastructural expenses by using already existing room illumination [18].

Fig. 3 presents the results on the achievable secrecy capacity and the corresponding consumed power for the NCPS scenario (under the assumption that the transmit nodes have the same fixed power levels). As it can be seen from Fig. 3a, the user can attain the required SC in the small area of the central part of the room while the achievable SC decreases as the user moves to the room edge. This can be also supported by Fig. 3b where the system consumes its maximum available

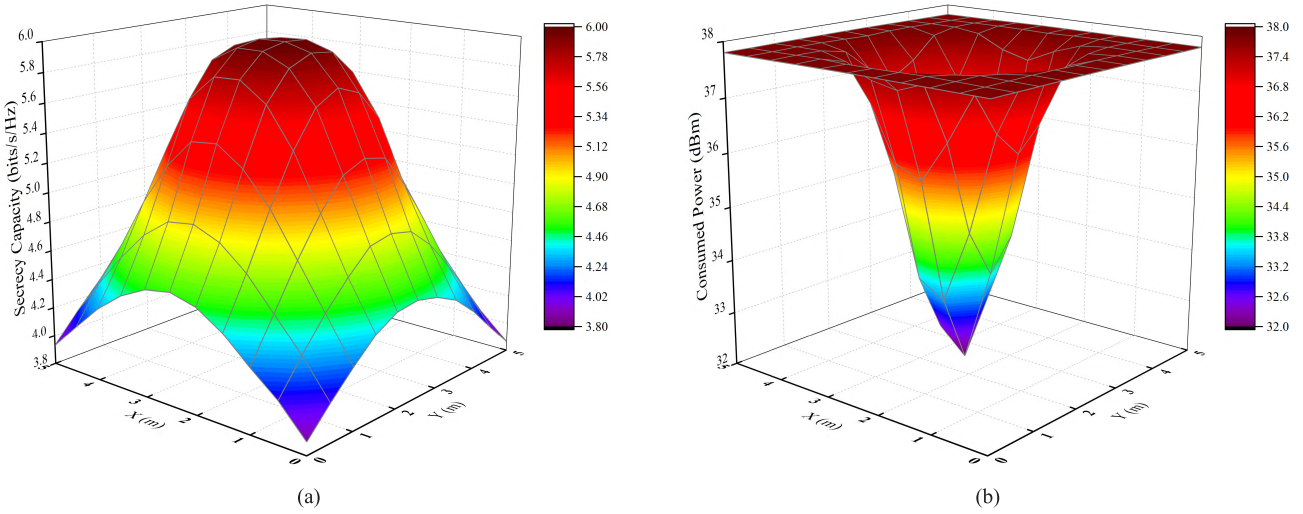

(a) (b)

FIGURE 3. The achievable secrecy capacity and consumed power of the hybrid non-cooperative scheme with respect to the room dimensions in the presence of E. (a) The achievable secrecy capacity. (b) The consumed power.

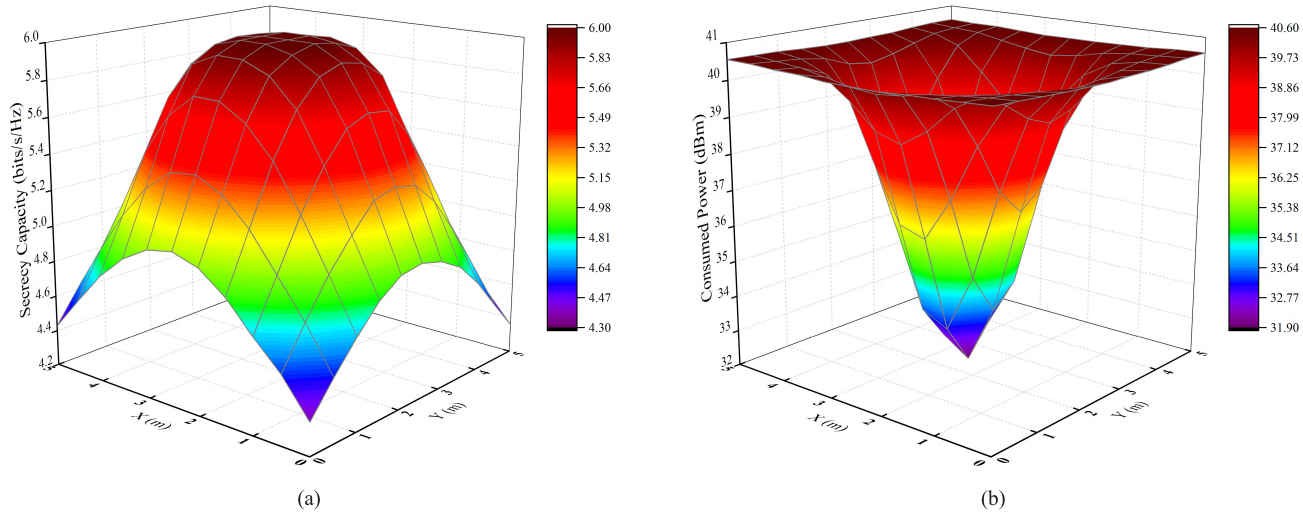

(a) (b)

FIGURE 4. The achievable secrecy capacity and consumed power of the hybrid cooperative scheme with respect to the room dimensions in the presence of E. (a) The achievable secrecy capacity. (b) The consumed power.

power by attempting to satisfy the required SC threshold. And the system consumes less power as the user moves toward to the room center, as expected. It is worthwhile mentioning that we consume less power at the locations of the source and relay nodes as it can be observed from Fig. 3b.

In the next plot, we demonstrate the results of the hybrid RF/VLC relaying system (see Fig. 4) under assumption that the transmit nodes are allowed to share the available power between each other (i.e., the CPS scenario). Compared to the previous results, we can notice that the proposed CPS case provides better SC coverage which comes at the price of a higher power consumption (refer to Figs. 4a and 4b). The power profile, similar to the NCPS scenario, can be noticed for the CPS case as well, i.e., less power is consumed in the center of the room.

Moreover, since the proposed CPS scenario achieves the best performance it is interesting to find out the impact of the individual components comprising the overall achievable SC presented in Fig. 4a. From Fig. 5, we can notice an asymmetry in the secrecy capacity outline where the system achieves less capacity at the location of E. This feature is more evident in the VLC component of the total secrecy capacity due to the deterministic nature of its channel as shown in Fig. 5b. On the other hand, the SC related to the RF component is less affected because it has a probabilistic channel model and the ZFBF is applied to mitigate the effect of E [37].

Fig. 6 shows some numerical results on the power consumption and achievable SC as a function of the target SC threshold for the standalone RF, standalone VLC, NCPS and CPS systems. in the following results, we fix the user location at a certain point $(x = 3, y = 3, z = 1)$ m in order to make a

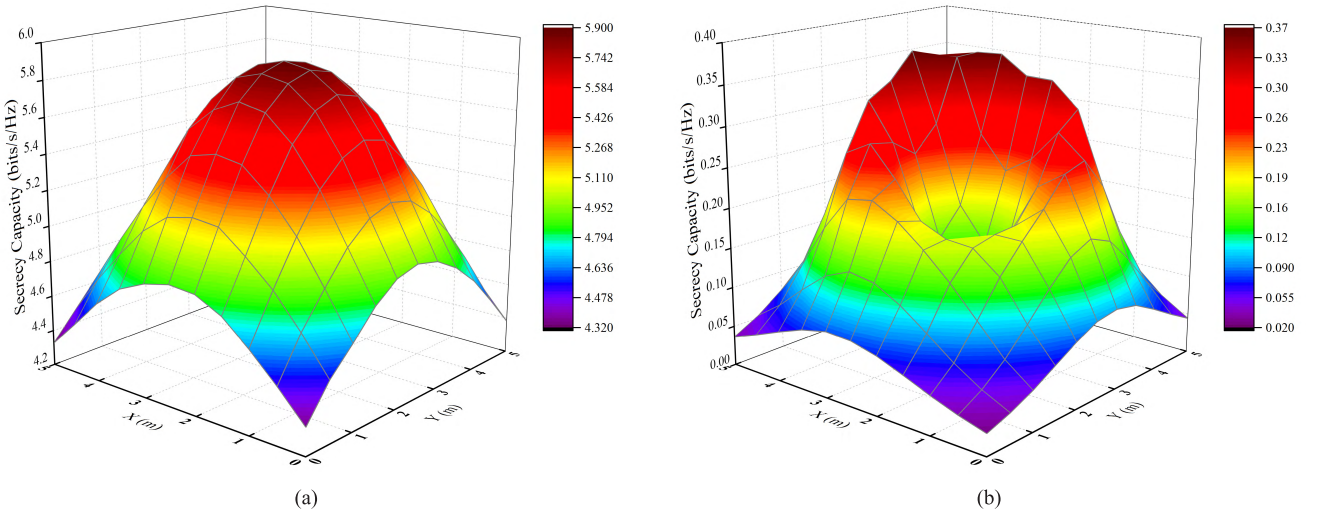

FIGURE 5. The achievable secrecy capacity of the hybrid cooperative scheme with respect to the room dimensions in the presence of E. (a) The RF component. (b) The VLC component.

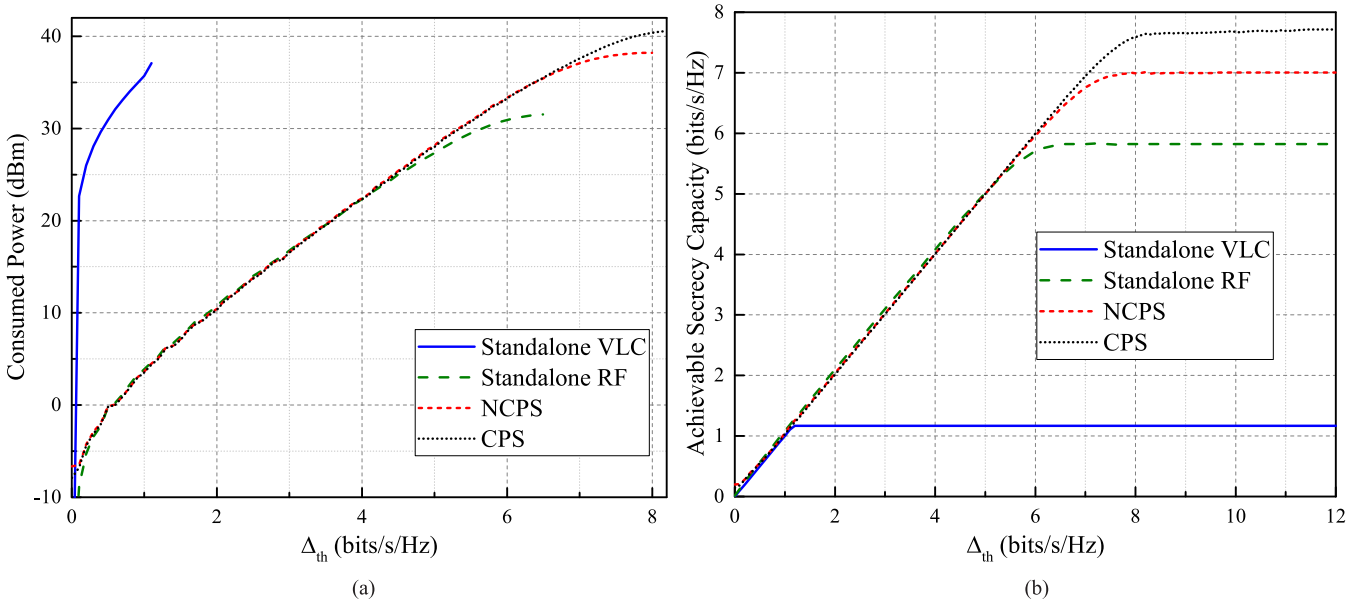

FIGURE 6. The consumed power and achievable secrecy capacity versus the SC threshold. (a) The consumed power. (b) The achievable secrecy capacity.

fair comparison. For instance, from Fig. 6a, we can notice that the consumed power of the standalone VLC briefly reaches its maximum at $\Delta_{\text{th}} = 1.1$ bits/s/Hz which also corresponds to the starting point of the saturation of the achievable secrecy capacity at 1.17 bits/s/Hz. On the other hand, the standalone RF system can be characterized by a gradual increase of the consumed power and secrecy capacity, and the saturation of both curves starts at $\Delta_{\text{th}} = 4.5$ bits/s/Hz and becomes constant at $\Delta_{\text{th}} = 6.5$ bits/s/Hz, respectively. Next, we consider the proposed NCPS scenario which can be described by a higher achievable secrecy capacity which maximum attains 7 bits/s/Hz at $\Delta_{\text{th}} = 8$ bits/s/Hz. This performance improvement is due to the hybrid nature of the proposed system model when the transmit nodes are restricted by fixed power levels. Moreover, we can observe that the NCPS policy does not utilize the whole available power because, due to the DF mode, S consumes less power compared to R to securely deliver the message to the user of interest. This occurs due to the configuration of the S-to-R link defined in Tables 2 and 3. Finally, we investigate the performance metrics typical to the CPS scenario when the nodes are allowed to share their available transmit power levels. It can be seen that the system can achieve higher SC and the permanent saturation happens after $\Delta_{\text{th}} = 8.2$ bits/s/Hz. This SC gain is attainable by a

TABLE 3. The VLC simulation parameters.

Parameter	Value
The location of S:	
S_1	$(x = 1.66, y = 1.66, z = 3)$ m
S_2	$(x = 1.66, y = 3.33, z = 3)$ m
S_3	$(x = 3.33, y = 1.66, z = 3)$ m
S_4	$(x = 3.33, y = 3.33, z = 3)$ m
The location of R:	
R_1	$(x = 2.45, y = 2.55, z = 2)$ m
R_2	$(x = 2.55, y = 2.55, z = 2)$ m
R_3	$(x = 2.45, y = 2.45, z = 2)$ m
R_4	$(x = 2.55, y = 2.45, z = 2)$ m
The order of Lambertian emission, m	1
Half irradiance semi-angle, $\phi_{\frac{1}{2}}$	60°
The detector's physical area, A	1 cm^2
Signal transmission of the filter, $T_s(\psi)$	1
The concentrator gain $g(\psi)$	1
The concentrator's field-of-view, Ψ_c	85°
Available power per node j, $P_{j_{max}}^{[\text{vlc}]}$, $j \in \{S, R\}$	0.3 Watt
Number of light fixtures per node, F	4
Number of LEDs per light fixture, N_i, $i \in \{S, R\}$	16
Noise power per node i, $\sigma_{n_i}^2$	2×10^{-15} A^2
Scaling factor, κ_j, $j \in \{S, R\}$	0.54 Watt/A
The PD responsivity, ρ_i, $i \in \{R, D, E\}$	0.8 A/Watt

means of the allowed power distribution between the transmit nodes. For instance, this can be explained by the fact that an optimal power distribution mechanism takes place in the CPS policy when redundant power available at one of the transmit nodes can be utilized by the other node to achieve the total SC requirement.

Fig. 7 demonstrates the results on the SOP of the proposed hybrid RF/VLC network deploying NCPS and CPS policies and for the standalone RF system. We can observe that the both proposed schemes outperform the standalone RF model. Moreover, the CPS scenario obtains the best outage probability and can be characterized by different SC gaps between the NCPS and CPS curves, from 0.2 bits/s/Hz to 0.76 bits/s/Hz. This change occurs at $\Delta_{\text{th}} = 6.7$ bits/s/Hz. This can be explained by the fact that the proposed CPS algorithm starts

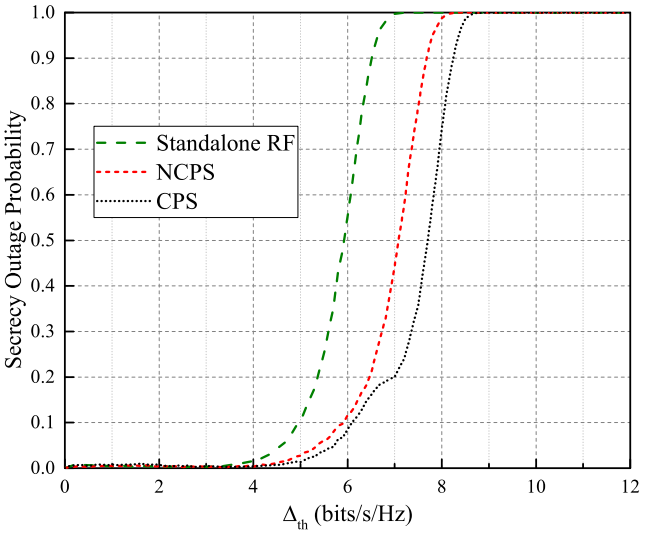

FIGURE 7. The SOP versus the total SC threshold.

distributing the power at this point in order to achieve higher secrecy capacity.

VII. CONCLUSION

In this paper, we studied the physical layer security aspects of the DF-based hybrid RF/VLC relaying system in the presence of the unauthorized user which is located in the same room with the legitimate receiver. We proposed two power saving policies (given by Algorithms 1 and 2), namely, NCPS and CPS. First, we obtained the BF vectors for the RF and VLC subsystems in order to maximize the achievable secrecy capacity by using the ZFBF technique to nullify the signal reception at E. Then we solved the power minimization problem satisfying our required secrecy capacity requirement by applying the obtained RF and VLC BF vectors. In the case of the NCPS policy, the transmit nodes are characterized by fixed power levels while, in the case of the CPS, the transmit nodes are restricted by a total power which can be shared between to achieve the SC requirement. Moreover, we numerically validated our proposed system model for the given RF and VLC parameters. The 3D results on the SC demonstrated that the CPS scenario outperforms the NCPS one. It also was shown that the SC performance is influenced by the location of E, i.e., the SC has a lower slope at the E's position, and this statement is valid for the both network policies. Furthermore, it was noticed that the NCPS consumes less power compared to the CPS due to the fact that the CPS has the ability to distribute the redundant power to achieve higher SC. Finally, the results showed that the CPS case has lower secrecy outage probability compared to the NCPS, and this is due to the fact that the CPS allows the nodes to share the power between the nodes while, in the NCPS, the power distribution is not applicable.

REFERENCES

[1] J. Reed, M. Vassiliou, and S. Shah, "The role of new technologies in solving the spectrum shortage," *Proc. IEEE*, vol. 104, no. 6, pp. 1163–1168, Jun. 2016.

[2] International Telecommunication Union. (Sep. 2017). *Broadband Catalyzing Sustainable Development*. [Online]. Available: https://www.itu.int/dms_pub/itu-s/opb/pol/S-POL-BROADBAND.18-2017-PDF-E.pdf

[3] J. Chapin and W. Lehr, "Mobile broadband growth, spectrum scarcity, and sustainable competition," in *Proc. 39th Res. Conf. Commun., Inf. Internet Policy*, Sep. 2011, pp. 1–11.

[4] M. Z. Chowdhury, M. T. Hossan, A. Islam, and Y. M. Jang, "A comparative survey of optical wireless technologies: Architectures and applications," *IEEE Access*, vol. 6, pp. 9819–9840, 2018.

[5] H. Haas, L. Yin, Y. Wang, and C. Chen, "What is LiFi?" *J. Lightw. Technol.*, vol. 34, no. 6, pp. 1533–1544, Mar. 15, 2016.

[6] A. Jovicic, J. Li, and T. Richardson, "Visible light communication: Opportunities, challenges and the path to market," *IEEE Commun. Mag.*, vol. 51, no. 12, pp. 26–32, Dec. 2013.

[7] T. Komine and M. Nakagawa, "Fundamental analysis for visible-light communication system using LED lights," *IEEE Trans. Consum. Electron.*, vol. 50, no. 1, pp. 100–107, Feb. 2004.

[8] H. Haas, "LiFi is a paradigm-shifting 5G technology," *Rev. Phys.*, vol. 3, pp. 26–31, Nov. 2018.

[9] P. K. Jha, N. Mishra, and D. S. Kumar, "Challenges and potentials for visible light communications: State of the art," in *Proc. AIP Conf.*, vol. 1849, Jun. 2017, pp. 020007-1–020007-8.

[10] M. Ayyash *et al.*, "Coexistence of WiFi and LiFi toward 5G: Concepts, opportunities, and challenges," *IEEE Commun. Mag.*, vol. 54, no. 2, pp. 64–71, Feb. 2016.

[11] D. A. Basnayaka and H. Haas, "Hybrid RF and VLC systems: Improving user data rate performance of VLC systems," in *Proc. IEEE 81st Veh. Technol. Conf. (VTC)*, May 2015, pp. 1–5.

[12] C. Yan, Y. Xu, J. Shen, and J. Chen, "A combination of VLC and WiFi based indoor wireless access network and its handover strategy," in *Proc. IEEE Int. Conf. Ubiquitous Wireless Broadband (ICUWB)*, Oct. 2016, pp. 1–4.

[13] R. Johri, "Li-Fi, complementary to Wi-Fi," in *Proc. Int. Conf. Comput. Power, Energy Inf. Commun. (ICCPEIC)*, Apr. 2016, pp. 15–19.

[14] X. Li, R. Zhang, and L. Hanzo, "Cooperative load balancing in hybrid visible light communications and WiFi," *IEEE Trans. Commun.*, vol. 63, no. 4, pp. 1319–1329, Apr. 2015.

[15] T. D. C. Little and M. Rahaim, "Network topologies for mixed RF-VLC HetNets," in *Proc. IEEE Summer Topicals Meeting Ser. (SUM)*, Jul. 2015, pp. 163–164.

[16] H. Chowdhury, I. Ashraf, and M. Katz, "Energy-efficient connectivity in hybrid radio-optical wireless systems," in *Proc. 10th Int. Symp. Wireless Commun. Syst. (ISWCS)*, Aug. 2013, pp. 1–5.

[17] T. Rakia, H.-C. Yang, F. Gebali, and M.-S. Alouini, "Optimal design of dual-hop VLC/RF communication system with energy harvesting," *IEEE Commun. Lett.*, vol. 20, no. 10, pp. 1979–1982, Oct. 2016.

[18] M. Kashef, M. Ismail, M. Abdallah, K. A. Qaraqe, and E. Serpedin, "Energy efficient resource allocation for mixed RF/VLC heterogeneous wireless networks," *IEEE J. Sel. Areas Commun.*, vol. 34, no. 4, pp. 883–893, Apr. 2016.

[19] J. Al-khori, G. Nauryzbayev, M. Abdallah, and M. Hamdi, "Secrecy capacity of hybrid RF/VLC DF relaying networks with jamming," in *Proc. Int. Conf. Comput., Netw. Commun. (ICNC)*, Honolulu, HI, USA, Feb. 2019, pp. 1–6.

[20] M. B. Rahaim *et al.*, "A hybrid radio frequency and broadcast visible light communication system," in *Proc. IEEE GLOBECOM Workshops (GC Wkshps)*, Dec. 2011, pp. 792–796.

[21] J. Mo, M. Tao, and Y. Liu, "Relay placement for physical layer security: A secure connection perspective," *IEEE Commun. Lett.*, vol. 16, no. 6, pp. 878–881, Jun. 2012.

[22] S. Arzykulov, G. Nauryzbayev, and T. A. Tsiftsis, "Underlay cognitive relaying system over α-μ fading channels," *IEEE Commun. Lett.*, vol. 21, no. 1, pp. 216–219, Jan. 2017.

[23] G. Nauryzbayev, S. Arzykulov, T. A. Tsiftsis, and M. Abdallah, "Performance of cooperative underlay CR-NOMA networks over Nakagami-m channels," Âİin *Proc. IEEE Int. Conf. Commun. Workshops (ICC Wkshps)*, May 2018, pp. 1–6.

[24] G. Nauryzbayev, K. M. Rabie, M. Abdallah, and B. Adebisi, "Ergodic capacity analysis of wireless powered AF relaying systems over α-μ fading channels," in *Proc. IEEE Global Commun. Conf. (Globecom)*, Dec. 2017, pp. 1–6.

[25] S. Arzykulov, G. Nauryzbayev, T. A. Tsiftsis, and M. Abdallah, "On the capacity of wireless powered cognitive relay network with interference alignment," Âİin *Proc. IEEE Global Commun. Conf. (Globecom)*, Dec. 2017, pp. 1–6.

[26] S. Arzykulov, G. Nauryzbayev, T. A. Tsiftsis, and M. Abdallah, "Error performance of wireless powered cognitive relay networks with interference alignment," in *Proc. IEEE 28th Annu. Int. Symp. Pers., Indoor, Mobile Radio Commun. (PIMRC)*, Oct. 2017, pp. 1–5.

[27] O. Narmanlioglu, R. C. Kizilirmak, F. Miramirkhani, and M. Uysal, "Cooperative visible light communications with full-duplex relaying," *IEEE Photon. J.*, vol. 9, no. 3, pp. 1–11, Jun. 2017.

[28] R. C. Kizilirmak and M. Uysal, "Relay-assisted OFDM transmission for indoor visible light communication," in *Proc. IEEE Int. Black Sea Conf. Commun. Netw. (BlackSeaCom)*, May 2014, pp. 11–15.

[29] H. Yang and A. Pandharipande, "Full-duplex relay VLC in LED lighting triangular system topology," in *Proc. 6th Int. Symp. Commun. Control Signal Process. (ISCCSP)*, May 2014, pp. 85–88.

[30] M. R. Zenaidi, Z. Rezki, M. Abdallah, K. A. Qaraqe, and M. S. Alouini, "Achievable rate-region of VLC/RF communications with an energy harvesting relay," in *Proc. IEEE Global Commun. Conf. (Globecom)*, Dec. 2017, pp. 1–7.

[31] T. Rakia, H.-C. Yang, F. Gebali, and M.-S. Alouini, "Dual-hop VLC/RF transmission system with energy harvesting relay under delay constraint," in *Proc. IEEE Globecom Workshops (Globecom Wkshps)*, Dec. 2016, pp. 1–6.

[32] M. Masoud, I. Jannoud, A. Ahmad, and H. Al-Shobaky, "The power consumption cost of data encryption in smartphones," in *Proc. Int. Conf. Open Source Softw. Comput. (OSSCOM)*, Sep. 2015, pp. 1–6.

[33] J. Wu, I. Detchenkov, and Y. Cao, "A study on the power consumption of using cryptography algorithms in mobile devices," in *Proc. 7th IEEE Int. Conf. Softw. Eng. Service Sci. (ICSESS)*, Aug. 2016, pp. 957–959.

[34] A. Mukherjee, S. A. A. Fakoorian, J. Huang, and A. L. Swindlehurst, "Principles of physical layer security in multiuser wireless networks: A survey," *IEEE Commun. Surveys Tuts.*, vol. 16, no. 3, pp. 1550–1573, Aug. 2014.

[35] Y. Zou, J. Zhu, X. Wang, and L. Hanzo, "A survey on wireless security: Technical challenges, recent advances, and future trends," *Proc. IEEE*, vol. 104, no. 9, pp. 1727–1765, Sep. 2016.

[36] J. Zhang, T. Q. Duong, A. Marshall, and R. Woods, "Key generation from wireless channels: A review," *IEEE Access*, vol. 4, pp. 614–626, 2016.

[37] M. F. Marzban, M. Kashef, M. Abdallah, and M. Khairy, "Beamforming and power allocation for physical-layer security in hybrid RF/VLC wireless networks," in *Proc. 13th Int. Wireless Commun. Mobile Comput. Conf. (IWCMC)*, Jun. 2017, pp. 258–263.

[38] L. Dong, Z. Han, A. P. Petropulu, and H. V. Poor, "Improving wireless physical layer security via cooperating relays," *IEEE Trans. Signal Process.*, vol. 58, no. 3, pp. 1875–1888, Mar. 2010.

[39] L. Dong, Z. Han, A. P. Petropulu, and H. V. Poor, "Cooperative jamming for wireless physical layer security," in *Proc. IEEE/SP 15th Workshop Statist. Signal Process.*, Aug. 2009, pp. 417–420.

[40] Y. Zou, X. Wang, and W. Shen, "Optimal relay selection for physical-layer security in cooperative wireless networks," *IEEE J. Sel. Areas Commun.*, vol. 31, no. 10, pp. 2099–2111, Oct. 2013.

[41] Y. Liu, J. Li, and A. P. Petropulu, "Destination assisted cooperative jamming for wireless physical-layer security," *IEEE Trans. Inf. Forensics Security*, vol. 8, no. 4, pp. 682–694, Apr. 2013.

[42] A. Mostafa and L. Lampe, "Physical-layer security for MISO visible light communication channels," *IEEE J. Sel. Areas Commun.*, vol. 33, no. 9, pp. 1806–1818, Sep. 2015.

[43] J. M. Kahn and J. R. Barry, "Wireless infrared communications," *Proc. IEEE*, vol. 85, no. 2, pp. 265–298, Feb. 1997.

[44] S. Leung-Yan-Cheong and M. E. Hellman, "The Gaussian wire-tap channel," *IEEE Trans. Inf. Theory*, vol. 24, no. 4, pp. 451–456, Jul. 1978.

[45] M. Kang and M.-S. Alouini, "A comparative study on the performance of MIMO MRC systems with and without cochannel interference," *IEEE Trans. Commun.*, vol. 52, no. 8, pp. 1417–1425, Aug. 2004.

[46] F. Oggier and B. Hassibi, "The secrecy capacity of the MIMO wire-tap channel," *IEEE Trans. Inf. Theory*, vol. 57, no. 8, pp. 4961–4972, Aug. 2011.

[47] S. Boyd and L. Vandenberghe, *Convex Optimization*, 7th ed. Cambridge, U.K.: Cambridge Univ. Press, 2004.

JABER AL-KHORI received the B.Sc. degree (Hons.) in electrical engineering from the University of Colorado at Denver, Denver, USA, in 2012, and the M.Sc. degree in telecommunications from Southern Methodist University, Dallas, USA, in 2014. He is currently pursuing the Ph.D. degree in computer science and engineering with Hamad Bin Khalifa University, Doha, Qatar. His research interests include wireless communication systems, with particular focus on visible light communication, relaying systems, anti-jamming techniques, and physical layer security.

Galymzhan Nauryzbayev (M'16) received the B.Sc. (Hons.) degree and M.Sc. (Hons.) degree in radio engineering, electronics and telecommunications from Almaty University of Power Engineering and Telecommunication, Almaty, Kazakhstan, in June 2009 and June 2011, respectively. In 2016, he obtained a Ph.D. degree in wireless communications from the University of Manchester and then started working as a Contracted Research Associate at Nazarbayev University, Astana, Kazakhstan. From 2016 to 2018, he held academic and research positions at L.N. Gumilyov Eurasian National University (Astana, Kazakhstan) and Hamad Bin Khalifa University (Qatar). In 2019, he joined Nazarbayev University (Astana, Kazakhstan) as an Assistant Professor. His research interest is in the area of wireless communication systems, with particular focus on multiuser MIMO systems, cognitive radio, signal processing, energy harvesting, visible light communications, NOMA, interference mitigation, etc. He is invited as a Guest Editor and Editorial board member for the *Special Issue Wireless Power Transfer Technology* in the open-access journal *Technologies* and open-access *International Journal of Wireless Communication and Sensor Networks*, respectively. Dr. Nauryzbayev served as a Technical Program Committee member on numerous IEEE flagship conferences.

MOHAMED M. ABDALLAH received the B.Sc. degree from Cairo University, in 1996, and the M.Sc. and Ph.D. degrees from the University of Maryland at College Park, in 2001 and 2006, respectively. From 2006 to 2016, he held academic and research positions at Cairo University and Texas A&M University, Qatar. He is currently a Founding Faculty Member with the rank of an Assistant Professor with the College of Science and Engineering, Hamad Bin Khalifa University. His current research interests include the design and performance of physical layer algorithms for cognitive networks, cellular heterogeneous networks, sensor networks, smart grids, visible light and free-space optical communication systems, and reconfigurable smart antenna systems. He was a recipient of the Nortel Networks Industrial Fellowship for five consecutive years, from 1999 to 2003, the Best Paper Award in the IEEE First Workshop on Smart Grid and Renewable Energy, in 2015, and the Research Fellow Excellence Award at Texas A&M University, in 2016.

Dr. Abdallah professional activities include a Technical Program Committee Member of several major IEEE conferences, a Technical Program Chair of the 10th International Conference on Cognitive Radio Oriented Wireless Networks, and an Associate Editor for the IEEE TRANSACTIONS ON COMMUNICATIONS.

MOUNIR HAMDI (S'89–M'90–SM'06–F'11) received the M.S. and Ph.D. degrees in electrical engineering from the University of Pittsburgh, Pittsburgh, PA, USA, in 1987 and 1991, respectively.

He was a Chair Professor with The Hong Kong University of Science and Technology (HKUST) and the Head of the Department of Computer Science and Engineering. He was a Founding Member of HKUST. From 1999 to 2000, he was a Visiting Professor with Stanford University, Stanford, CA, USA, and the Swiss Federal Institute of Technology, Lausanne, Switzerland. He is currently the Founding Dean of the College of Science and Engineering, Hamad Bin Khalifa University, Doha, Qatar. In addition, he has frequently consulted for companies and governmental organizations in the USA, Europe, and Asia. His research interest includes high-speed wired/wireless networking. He has authored or co-authored more than 300 research publications in the above area. His contributions include design and analysis of high-speed packet switching.

Prof. Hamdi was a member of the ComSoc Technical Activities Council. He was a recipient of the Best Paper Award of the IEEE International Conference on Information and Networking, in 1998, the IEEE International Conference on Communications, in 2009, and the IEEE GLOBECOM, in 2011. He also supervised the Best Ph.D. Paper Award amongst all universities in Hong Kong. He was a recipient of the Best Ten Lecturers Award of HKUST. He has chaired more than 20 international conferences and workshops. He was the Chair of the IEEE Communications Society Technical Committee on Transmissions, Access and Optical Systems, and the Vice-Chair of the Optical Networking Technical Committee. He has been on the Editorial Board of various prestigious journals and magazines including the IEEE TRANSACTIONS ON COMMUNICATIONS, the *IEEE Communication Magazine*, *Computer Networks*, *Wireless Communications and Mobile Computing*, and *Parallel Computing*, a Guest Editor for the *IEEE Communications Magazine*, the Guest Editor-in-Chief of two special issues of the IEEE JOURNAL ON SELECTED AREAS OF COMMUNICATIONS, and a Guest Editor for the *Optical Networks Magazine*. He is also a frequent keynote speaker at international conferences and forums.